

Positron emission tomographic imaging with ^{11}C -choline in differential diagnosis of head and neck tumors: comparison with ^{18}F -FDG PET

Nasim KHAN,* Noboru ORIUCHI,* Hiroshi NINOMIYA,** Tetsuya HIGUCHI,*
Hideo KAMADA** and Keigo ENDO*

*Department of Nuclear Medicine & Diagnostic Radiology, and **Department of Head and Neck Surgery,
Gunma University, Faculty of Medicine

The aim of this study was to evaluate the clinical value of positron emission tomography (PET) with ^{11}C -labeled choline (CHOL) for the differential diagnosis of malignant head and neck tumors from benign lesions as compared with ^{18}F -fluorodeoxyglucose PET. **Methods:** We studied 45 patients (28 males, 17 females, age range, 29–84 years) with suspected lesions in the head and neck region using both CHOL and FDG PET within a 2-week period on each patient. All patients fasted for at least 6 hours for both the CHOL and FDG studies. PET imaging was performed 5 min and 50–60 min after intravenous injection of CHOL and FDG, respectively. After data acquisition, PET images were corrected for attenuation, and the reconstructed images were analyzed by visual interpretation. Then, the standardized uptake value (SUV) was calculated for semiquantitative evaluation of tumor tracer uptake. Finally the results of PET scans were compared with the histological diagnoses from surgical specimens or biopsies. **Results:** With CHOL PET, malignant tumors were correctly detected in 24 (96%) of 25 patients, and benign lesions in 14 (70%) of 20 patients with an accuracy of 84.4%. With FDG PET, malignancy was correctly diagnosed in 23 (92%) of 25 patients, and benign lesions in 13 (65%) of 20 patients resulting an accuracy of 80%. A significant positive correlation between CHOL and FDG SUVs was found for all lesions ($r = 0.677$, $p = 0.004$, $n = 45$). Malignant tumors showed significantly higher tracer accumulation than the benign lesions in both CHOL and FDG studies (5.69 ± 1.61 , $n = 25$ vs. 2.98 ± 2.13 , $n = 20$, $p < 0.0001$; 9.21 ± 4.23 , $n = 25$ vs. 3.60 ± 2.57 , $n = 20$, $p < 0.0001$). The cutoff SUV for differentiating malignant and benign lesions was 3.5 for CHOL and 3.9 for FDG. CHOL showed slightly better differentiation between malignant and benign lesions than FDG although some overlap existed on both studies. But the difference was not statistically significant. **Conclusion:** The results of this study indicate that CHOL PET may be feasible clinically for head and neck tumor imaging. PET imaging with CHOL seems to be able to detect malignant head and neck tumors as effectively as FDG PET. The advantages of CHOL PET were shorter examination period and low uptake in the muscle. However, both CHOL and FDG have some limitations in the evaluation of salivary gland lesions.

Key words: PET, CHOL, FDG, head and neck tumors, SUV

INTRODUCTION

MALIGNANT TUMORS of the head and neck region are often potentially curable by locoregional treatment if they are diagnosed at an early stage.¹ Therefore, the early detection and accurate differentiation between malignant and benign mass lesions is important when such differentiation is difficult clinically for planning appropriate therapy. For this purpose, in many instances, the conventional imaging techniques such as computed tomography (CT),

Received January 28, 2004, revision accepted March 30, 2004.

For reprint contact: Nasim Khan, M.D., Department of Nuclear Medicine and Diagnostic Radiology, Gunma University, Faculty of Medicine, 3–39–22 Showamachi, Maebashi, Gunma 371–8511, JAPAN.

E-mail: nasim@med.gunma-u.ac.jp

magnetic resonance imaging (MRI) and ultrasonography (US) are of limited accuracy.² Consequently, there is a great need for a high technology noninvasive imaging method that allows the detection of head and neck malignancy more accurately.

Positron emission tomography (PET) has been successfully used for the evaluation of a variety of cancers including head and neck cancer, complementing or simply demonstrating greater accuracy than the morphological imaging modalities.^{3,4} The use of PET for the diagnosis of cancer in the human body is based on the unique capability of this technique to evaluate metabolic activity in neoplasm. The glucose analog ¹⁸F-fluorodeoxyglucose (FDG) is rapidly transported into tumor cells, where it is phosphorylated and metabolically trapped as FDG-6-phosphate,⁵ which is the reason for the radioactivity accumulation in tumor hot spots on FDG PET imaging. PET imaging with FDG has shown promising results in the detection of head and neck malignancies by localizing regions of accelerated glucose metabolism that are highly correlated with malignancy.⁶ However, FDG is also accumulated in some benign lesions,⁷⁻⁹ and sometimes in muscle which may cause false-positive results. Another disadvantage of FDG PET imaging is that tumor FDG uptake is impaired in hyperglycemic conditions.¹⁰ Therefore, new radiotracers capable of overcoming these drawbacks in PET imaging and providing more sensitivity and specificity would be welcome.

Recently, a new PET tracer, carbon-11-choline (CHOL) has been developed as a tumor-detecting radiotracer for PET imaging,¹¹ and may be able to become a suitable PET tracer for head and neck tumor imaging. Unlike glucose, choline (an essential element of phospholipids) is incorporated into cells through phosphorylcholine synthesis and is integrated in membrane phospholipids.¹² It has been suggested that malignant transformation of cells is associated with the induction of choline kinase activity resulting in increased levels of phosphorylcholine for the synthesis of membrane phospholipids.¹³ It is also known that rapidly proliferating tumors contain large amounts of phospholipids, particularly phosphatidylcholine.¹⁴ An elevated level of phosphorylcholine in various cancers, has been revealed by both *in vitro* and *in vivo* magnetic resonance spectroscopy (MRS) studies, while in corresponding normal tissues the choline metabolite is present at low or undetectable levels.^{15,16} This provides the rationale for the use of CHOL in oncologic PET imaging. Several clinical studies have shown the usefulness of CHOL PET in different types of tumors such as brain tumors, esophageal cancer and prostate cancer.¹⁷⁻¹⁹ To our knowledge, there has been no previous study of head and neck tumor imaging with CHOL PET. Therefore, we had undertaken this study to investigate the feasibility of CHOL PET in head and neck tumor imaging as compared with FDG PET.

MATERIALS AND METHODS

Patients

Patients were recruited from among those referred to our department for PET imaging from the departments of Head and Neck Surgery and Oral Surgery of Gunma University Hospital, Gunma, Japan. We studied a consecutive series of 45 patients (28 men, 17 women; age range, 29–84 years, mean age, 61.64 years) with head and neck lesions. All patients who were referred for PET had an inconclusive diagnosis on clinical and radiologic examinations, and PET was performed to determine further diagnostic and therapeutic approach. Patients remained untreated until the PET study completed. Forty-five different lesions of maxillary and ethmoid sinuses, nasal cavity, tongue, pharynx, larynx, neck, parotid and submandibular glands were evaluated in the 45 patients studied.

After PET examination, the histological diagnosis was obtained in all patients studied within 1–2 wk by operation (n = 30) or biopsy (n = 15). Twenty-five patients had malignant tumors (22 primary tumors, 2 recurrent carcinoma and 1 metastatic carcinoma), including squamous cell carcinomas (n = 16), malignant lymphomas (n = 6), adenosquamous cell carcinoma (n = 1), basal cell carcinoma (n = 1) and poorly differentiated carcinoma (n = 1). The size of the lesions was determined from the resected specimens or CT and/or MRI scans and ranged from 0.9 to 4.7 cm. Twenty patients had benign lesions of different histological varieties (Table 1). We did not evaluate lymph node metastasis in this study because of the limited number of specimens. None of the patients had diabetes mellitus. Blood glucose levels in the patients studied ranged from 64 to 95 mg/dl (3.5–5.3 mmol/l).

The study protocol was approved by the Institutional Review Board of Gunma University Hospital, Gunma, and informed consent was obtained from all patients who participated in the study.

Synthesis of radiopharmaceuticals

Both CHOL and FDG were produced in-house using the cyclotron facility of Gunma University Hospital. CHOL was synthesized by the reaction of ¹¹C-methyl iodine with dimethylaminoethanol according to Hara et al.¹¹ Fluorine-18 was produced by a ²⁰Ne(d, α)¹⁸F nuclear reaction, and FDG was synthesized by the acetyl hypofluorite method with minor modifications of the previously described method by Hamacher et al.²⁰

Radionuclide purity of each compound was checked by high performance liquid chromatography and found to be greater than 97.9%.

PET imaging

PET studies were performed with a dedicated PET scanner (SET 2400W, Shimadzu, Kyoto, Japan) operated in 2D-mode. The scanner possesses whole-body imaging

Table 1 Patient characteristics and results of PET imaging in 45 head and neck lesions

Patient	Age (yr)	Sex (M/F)	Site of lesion	Lesion size (cm)	Histologic diagnosis	CHOL PET		FDG PET		Method of diagnosis
						Visual score	SUV	Visual score	SUV	
Malignant Lesions (n = 25)										
1	73	M	Carotid space l	2.5	Adenosquamous carcinoma	++	9.5	++	9.9	Ope
2	55	M	Maxillary sinus r	ND	Squamous cell carcinoma	++	8.8	++	10.4	Ope
3	64	F	Neck r	2.1	Poorly diff. carcinoma	++	8.2	++	11.4	Biopsy
4	74	M	Tonsil r	1.6	Basal cell carcinoma	++	7.7	++	10.1	Biopsy
5	54	M	Maxillary sinus r	3.9	Squamous cell carcinoma	++	7.6	++	17.6	Biopsy
6	53	M	Carotid space l	5.1	Squamous cell carcinoma	++	6.7	++	14.6	Ope
7	84	F	Tongue	2.1	Squamous cell carcinoma	++	6.2	++	6.1	Biopsy
8	60	M	Tongue	1.5	Squamous cell carcinoma	++	6.1	++	9.3	Ope
9	71	M	Tongue	3.2	Squamous cell carcinoma	++	5.7	++	5.5	Biopsy
10	77	F	Tonsil r	1.8	Squamous cell carcinoma	++	5.7	++	14.8	Ope
11	78	M	Hypopharynx	2.2	Squamous cell carcinoma	++	5.6	++	6.8	Biopsy
12	65	M	Hypopharynx	3.1	Squamous cell carcinoma	++	5.6	++	11.1	Biopsy
13	75	M	Submandibular gland r	4.3	Squamous cell carcinoma	++	5.4	++	6.3	Biopsy
14	72	M	Neck l	3.7	Squamous cell carcinoma	++	5.1	++	8.7	Ope
15	59	M	Hypopharynx	2.1	Squamous cell carcinoma	++	5.1	++	8.6	Biopsy
16	81	F	Tongue	3.1	Squamous cell carcinoma	++	5.1	++	7.9	Biopsy
17	56	M	Neck r	1.8	Lg malignant lymphoma	++	5.1	±	1.7	Ope
18	53	M	Parapharyngeal space l	1.5	Malignant lymphoma	++	4.7	++	11.3	Ope
19	74	F	Neck r	2.8	Malignant lymphoma	++	4.5	++	16.4	Ope
20	53	F	Neck l	2.2	Malignant lymphoma	++	4.5	+	4.9	Ope
21	71	F	Epipharynx r	2.5	Malignant lymphoma	+	4.2	++	12.4	Biopsy
22	67	M	Larynx	0.9	Squamous cell carcinoma	+	4.2	+	3.9	Biopsy
23	81	M	Tongue	1.5	Malignant lymphoma	+	3.9	++	13.5	Biopsy
24	81	M	Larynx	1.2	Well diff. Sq cell carcinoma	+	3.6	±	2.9	Biopsy
25	62	M	Submandibular gland r	2.1	Squamous cell carcinoma	±	3.4	+	4.2	Ope
Benign Lesions (n = 20)										
26	76	M	Parotid gland l	2.5	Warthin's tumor	++	7.3	++	8.2	Ope
27	63	M	Submandibular gland r	2.5	Chronic sialoadenitis	++	7.1	+	4.8	Ope
28	71	M	Parotid gland l	2.1	Warthin's tumor	++	6.7	++	10.1	Ope
29	29	M	Epipharynx r	1.7	Lymphoid hyperplasia	++	5.1	++	6.2	Biopsy
30	51	F	Parotid r	2.1	Pleomorphic adenoma	+	3.6	±	3.6	Ope
31	35	M	Sphenoid bone	3.9	Fibrous dysplasia	+	3.5	+	3.9	Ope
32	60	F	Parotid gland l	2.3	Granuloma	±	3.4	±	3.4	Ope
33	40	M	Parotid gland l	2.2	Pleomorphic adenoma	±	3.1	±	3.4	Ope
34	41	M	Nasal cavity r	2.5	Nasal polyp	±	2.9	±	1.6	Ope
35	58	F	Sphenoid sinus r	1.9	Mycotic sinusitis	±	2.9	±	2.4	Ope
36	50	F	Parotid r	1.9	Pleomorphic adenoma	±	2.5	++	6.4	Ope
37	54	F	Submandibular gland r	1.4	Pleomorphic adenoma	±	2.4	±	2.2	Ope
38	49	M	Parotid r	2.6	Pleomorphic adenoma	±	2.1	±	3.2	Ope
39	66	F	Parotid gland l	2.1	Pleomorphic adenoma	±	1.9	±	3.8	Ope
40	40	F	Parapharyngeal space l	4.5	Pleomorphic adenoma	±	1.7	+	4.2	Ope
41	82	F	Nasal cavity l	2.9	Cavernous hemangioma	±	1.1	±	2.1	Ope
42	62	M	Maxillary sinus r	1.8	Squamous papilloma	-	0.7	-	0.6	Ope
43	32	M	Maxillary sinus l	ND	Chronic sinusitis	-	0.6	-	0.7	Ope
44	78	F	Submandibular gland r	ND	Chronic sialoadenitis	-	0.5	-	0.4	Ope
45	44	F	Parotid r	4.7	Pleomorphic adenoma with cystic change	-	0.4	-	0.7	Ope

M = male, F = female, r = right, l = left, ND = not determined, diff. = differentiated, Lg = low-grade, Sq = squamous, - = negligible uptake, ± = mild uptake, + = moderate uptake, ++ = marked uptake, Ope = operation

Table 2 Comparison of CHOL and FDG PET results for the diagnosis of malignant head and neck tumors in 45 patients

	TP	FN	TN	FP	Sensitivity (%)	Specificity (%)	Accuracy (%)
CHOL PET	24	1	14	6	96	70	84.4
FDG PET	23	2	13	7	92	65	80

TP = true-positive, FN = false-negative, TN = true-negative, FP = false-positive

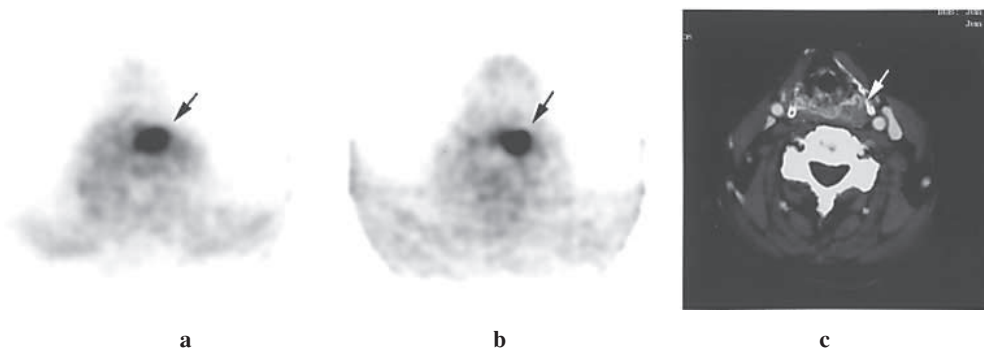


Fig. 1 Patient 11. Hypopharyngeal carcinoma. The tumor is as clearly visualized (*arrow*) in CHOL PET (a) as in the FDG PET study (b). The SUVs of the tumor with CHOL and FDG were 5.6 and 6.8, respectively. (c) Corresponding CT scan shows the tumor on the left side of the hypopharynx with inhomogeneous enhancement (*arrow*).

capability which images 63 planes at 3.125 mm intervals at one session. The diameter of the field-of-view is 59.5 cm and the axial length 20.0-cm. Patients fasted for at least 6 hours or overnight for both the CHOL and FDG PET studies. Drinking of water was allowed ad libitum. For the evaluation of the tumor depictability with both tracers in patients with head and neck lesions, images were obtained 5 minutes after the injection of 7–8 MBq/kg body weight of CHOL, and 50–60 minutes after the injection of 5–6 MBq/kg of FDG intravenously. After the radiotracer injection, the patients were instructed not to chew or talk, particularly during image acquisition. Static emission scans were acquired of the head and neck region using a one bed position for each patient routinely. In addition, whole-body scanning was performed in a few patients with a high probability of distant metastases (5–6 bed positions). In all cases, FDG PET was performed within 2 weeks of the CHOL PET study. Simultaneous emission and transmission data were acquired for 5 min for CHOL PET and 8 min for FDG PET at a bed position with a rotating external source (370 MBq $^{68}\text{Ge}/^{68}\text{Ga}$ at installation) for attenuation correction. The ordered-subsets expectation maximization (OSEM) iterative algorithm was used to produce transaxial PET images. The OSEM algorithm processes the data in subsets within each iteration; this procedure accelerates convergence by a factor proportional to the number of subsets. Attenuation-corrected transaxial images with CHOL and FDG were reconstructed into 128×128 matrices with pixel dimensions of 4.0 mm in-plane and 3.125 mm axially. Coronal images with a 9.8-mm slice thickness were

produced by using transaxial images. Both transaxial and coronal images were used for the visual assessment.

Data analysis

The PET images were visually interpreted by two independent nuclear medicine physicians from a direct digital display on a color-coded computer monitor; black and white hard-copy images were also available. Any disagreement was resolved by consensus. For qualitative analysis, abnormalities were defined as areas with tracer uptake above the normal level in comparison to the normal contralateral side or surrounding tissues. Visible uptake in the lesions was scored as negligible (–), mild (\pm), moderate (+) and marked (++) . All lesions with a moderate or marked uptake were defined as positive for the depiction of malignant tumors, and lesions with negligible or mild uptake were defined as negative results. An initial judgment of the PET scan readings was made with information on the site of clinical suspicion but without knowledge about the current CT and/or MRI findings. Finally all PET findings were compared with CT and/or MR images, and histological diagnoses.

For semiquantitative analysis of tumor tracer accumulation, functional images of the standardized uptake value (SUV) were produced using attenuation-corrected transaxial images, injected doses of CHOL and FDG, patient's body weight, and cross-calibration factors between the PET scanner and the dose calibrator. SUV was defined as follows: $\text{SUV} = \text{tissue concentration (MBq/g)} / (\text{injected dose [MBq]} / \text{body weight [g]})$.

For the assessment of tumor uptake of CHOL and FDG,

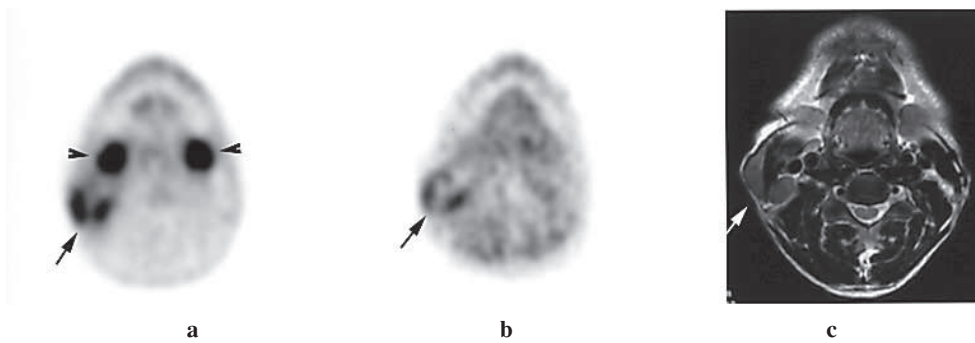


Fig. 2 The low-grade malignant lymphoma (*arrow*) of Patient 17 is more clearly visualized in the CHOL study (a) than in the FDG study (b). There is marked uptake of CHOL in the tumor (SUV, 5.1) consistent with true-positive diagnosis whereas the FDG uptake is low (SUV, 1.7) leading to a false-negative diagnosis. Physiologic uptake of CHOL is seen in bilateral submandibular glands (*arrowhead*). (c) Corresponding T1-weighted MR image demonstrates two adjoining soft tissue mass lesions (*arrow*) on the right side of the neck.

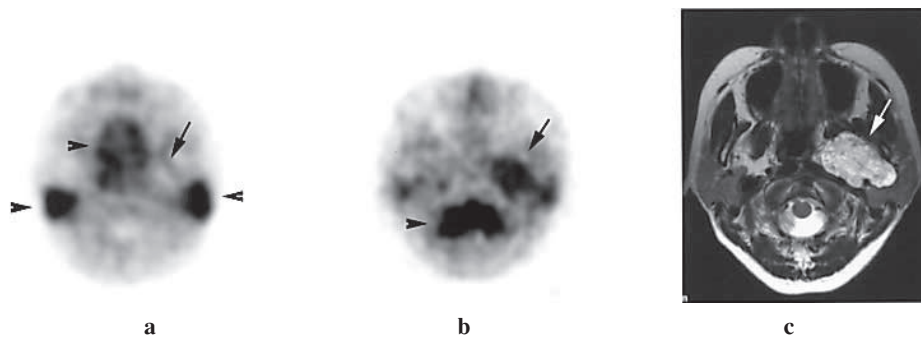


Fig. 3 Patient 40. Pleomorphic adenoma. CHOL PET (a) shows very low uptake in the corresponding tumor area (*arrow*) (SUV, 1.7) consistent with the true-negative diagnosis while FDG PET (b) shows moderately increased uptake (*arrow*) (SUV, 4.2) leading to a false-positive diagnosis. Physiologic uptake of CHOL is seen in the nasal mucosa and bilateral parotid glands (*arrowheads*). High normal uptake of FDG is also visualized in the cerebellum (*arrowhead*) in this image. (c) Corresponding T2-weighted MR image shows a hyperintense signal mass (*arrow*) in the left parapharyngeal space (4.5 cm).

regions of interest (ROIs) 1 cm in diameter were manually drawn on the SUV images over the area corresponding to the tumors in all lesions, which included the site of maximal radiotracer uptake. ROI analysis was conducted by a radiologist cum nuclear physician with the aid of corresponding CT scans and/or MR images. The average SUV within an ROI was used to represent the tumor uptake of CHOL and FDG.

Statistical analysis

The relationship between the CHOL and FDG SUVs for the lesions was assessed by linear regression analysis. Differences in mean SUVs for both CHOL and FDG between malignant and benign lesions were analyzed for statistical significance by two-tailed Student's *t* test for unpaired data. The sensitivity and specificity of CHOL PET were compared with those of FDG PET using Fisher's exact test. A *p* value < 0.05 was considered statistically significant.

RESULTS

Table 1 summarizes the results of PET imaging and the final diagnoses of the 45 patients studied. Sensitivity, specificity and accuracies are summarized in Table 2.

Of 25 lesions in 25 patients proved at histological examinations to be malignant, 22 were accurately diagnosed with both CHOL and FDG PET. A representative case of both CHOL and FDG true-positive is shown in Figure 1. In two patients with malignant tumors, CHOL PET could clearly detect 1 low-grade malignant lymphoma of the right neck (patient 17) and 1 well differentiated squamous cell carcinoma of the larynx (patient 24) whereas FDG PET was false-negative, probably because of their low-grade characteristic. A representative case is shown in Figure 2. On the other hand, CHOL PET was false-negative in 1 patient with metastatic squamous cell carcinoma in the right submandibular gland while FDG

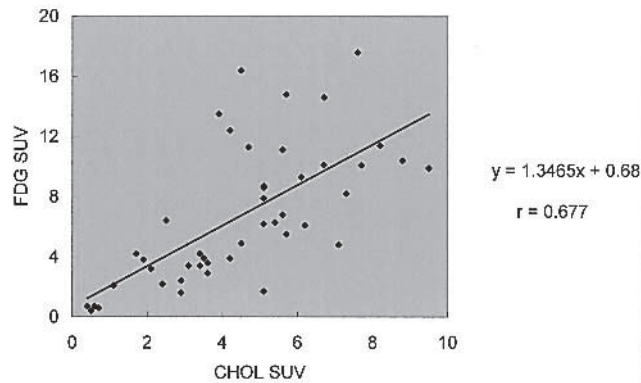


Fig. 4 Plot shows correlation between uptake of CHOL and FDG measured as SUV in head and neck tumors. A significant positive correlation is observed between SUVs of CHOL and FDG in all lesions ($r = 0.677$, $p = 0.004$, $n = 45$).

PET was true-positive, probably due to interference by relatively high physiologic CHOL uptake (patient 25), which is known from previous studies,^{21,22} and was also observed in our study.

CHOL PET was true-negative in 14 of 20 benign lesions whereas FDG PET revealed benignancy in 13 cases. Both tracers were false-positive in five cases: two Warthin's tumors (patient 26, 28), one chronic active sialoadenitis (patient 27), one reactive lymphoid hyperplasia (patient 29) and one fibrous dysplasia (patient 31). In two patients with pleomorphic adenomas (patient 36, 40), CHOL PET was true-negative whereas FDG PET was false-positive. A representative case is shown in Figure 3. However, CHOL PET could not exclude malignancy clearly in 1 patient with pleomorphic adenoma of the right parotid in which FDG PET was true-negative (patient 30).

The SUVs of CHOL ranged from 0.4 to 9.5 with a mean of (4.48 ± 2.29 , $n = 45$) for all lesions. SUVs of FDG ranged from 0.4 to 17.6 with a mean of (6.72 ± 4.55 , $n = 45$). The comparison between CHOL and FDG SUVs was performed by means of a scattergram (Fig. 4). A significant positive correlation was found between CHOL and FDG SUVs for all lesions ($r = 0.677$, $p = 0.004$, $n = 45$). The mean SUVs of CHOL and FDG between malignant tumors and benign lesions were (5.69 ± 1.61 , $n = 25$ vs. 2.98 ± 2.13 , $n = 20$) and (9.21 ± 4.23 , $n = 25$ vs. 3.60 ± 2.57 , $n = 20$), respectively. Mean SUV of CHOL was significantly lower than that of FDG in malignant lesions (5.69 ± 1.61 , $n = 25$ vs. 9.21 ± 4.23 , $n = 25$, $p = 0.0003$) in this study. But the difference of mean SUVs between malignant tumors and benign lesions were statistically significant with both tracers ($p < 0.0001$) (Fig. 5). CHOL showed better differentiation between malignant and benign lesions than FDG (Fig. 5a), although some overlap existed on both studies. Because of a significant difference in mean SUV of CHOL between malignant and benign lesions and relatively better differentiation ca-

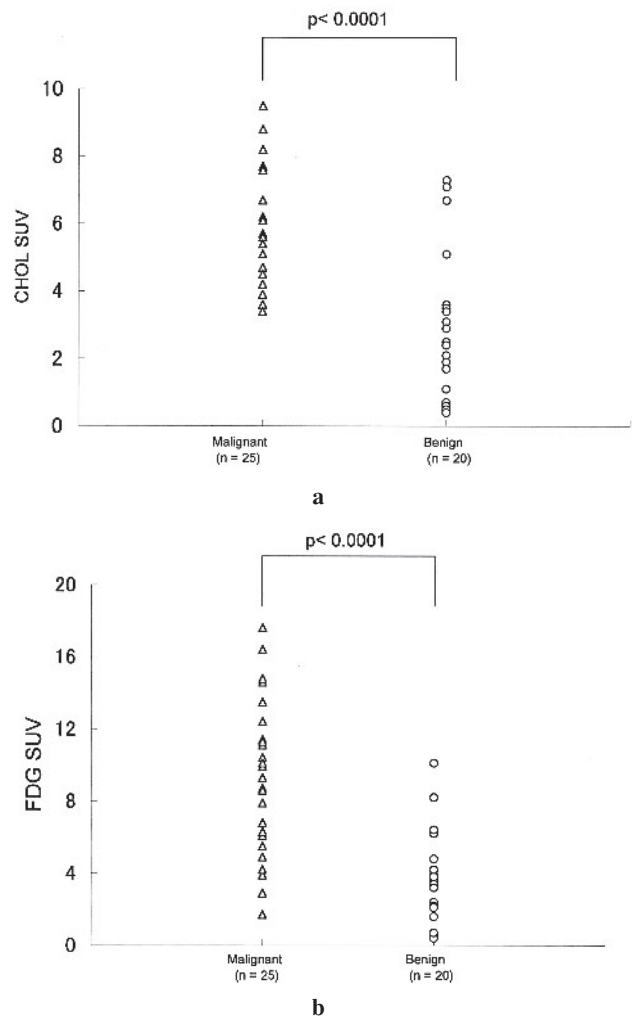


Fig. 5 Plots show CHOL (a) and FDG (b) uptake in tissues presented as SUVs in malignant ($n = 25$) and benign ($n = 20$) lesions. Both CHOL and FDG reveal significantly higher mean SUV in malignant tumors than benign lesions (5.69 ± 1.61 , $n = 25$ vs. 2.98 ± 2.13 , $n = 20$, $p < 0.0001$; and 9.21 ± 4.23 , $n = 25$ vs. 3.60 ± 2.57 , $n = 20$, $p < 0.0001$), respectively. Although some overlap exists on both tracers, CHOL shows better differentiation between malignant and benign lesions than FDG.

pability, CHOL PET seemed to be able to differentiate malignant head and neck tumors from benign disease as effectively as FDG. When an SUV of 3.5 was set for differentiating between malignant and benign lesions, all malignant tumors except one showed an increased SUV above the cutoff value with CHOL. With a cutoff value of 3.9, FDG PET could differentiate correctly 23 of 25 malignant tumors from benign lesions which well reflected the qualitative interpretation also. In terms of the diagnostic performance on a patient-by-patient basis, the sensitivity, specificity and accuracy of CHOL PET were 96%, 70% and 84.4%, respectively. The corresponding results for FDG PET were 92%, 65% and 80% (Table 2).

DISCUSSION

Although CHOL PET has shown significant potential for the detection and staging of tumors in the brain and prostate, organs in which FDG PET lacks sensitivity,^{17,19} to date no study has reported its application in head and neck tumor imaging. Our study was an initiative to evaluate the feasibility of CHOL PET in head and neck tumor imaging. For the detection of head and neck malignancy in 25 patients, CHOL and FDG PET were equally accurate in 22 patients including 20 primary malignant tumors and 2 recurrent tumors. In only 1 patient, CHOL PET could not clearly visualize a metastatic carcinoma in the submandibular gland (patient 25), probably because it was obscured by the relatively high tracer uptake in normal tissues. On the other hand, in two patients, only CHOL PET could clearly detect the malignancy. In 1 patient with a low-grade lymphoma, the tumor showed low FDG uptake (Fig. 2). In another patient with well differentiated laryngeal carcinoma, FDG could not clearly differentiate malignant tumor from benign lesion (patient 24). This might be due to the ability of CHOL to study different biologic activity that is not competitive with FDG. The uptake of CHOL in tumors represents cell membrane synthesis and probably tumor cell proliferation also,²³ whereas FDG uptake represents glycolysis. It is well known that FDG PET has a limited role in the diagnosis of low-grade malignant tumors,^{24,25} probably due to low glycolytic activity. In addition, tumor hypoxia which is often associated with large and high grade tumors also has an additional effect on increased cellular uptake of FDG.²⁶ In contrast, it is assumed that whether tumor cells are in hypoxia or in normoxia, the rate of CHOL uptake in tumors is an indicator of the tumor cell proliferation rate.²⁷ However, the relationship between intracellular choline metabolism and cellular proliferation rate remains to be established by further investigation. Although the mechanism of cellular incorporation of choline has not been completely clarified, 2 transport mechanisms have been suggested in mammalian cells: energy-dependent transmembrane transport and simple diffusion,^{14,28} phosphorylation also thought to be essential for metabolic retention of choline within cancer cells.²⁹

In the present study, we observed six false-positive cases with CHOL PET and seven cases with FDG PET. The false-positive cases on both CHOL and FDG PET were: 2 Warthin's tumors, 1 of 4 chronic inflammations, 1 fibrous dysplasia and 1 lymphoid hyperplasia. Among the three false-positive cases of pleomorphic adenomas, CHOL PET could exclude malignancy clearly in two cases whereas FDG PET could not differentiate benignancy clearly from malignant tumors (Fig. 3). But in one case CHOL showed relatively higher uptake whereas FDG PET was true-negative. Increased accumulation of CHOL in some inflammatory and benign reactive tissues has also been reported in several recent publications.^{27,30,31}

It has been suggested that both malignant and benign lesions are often infiltrated by macrophages and other immunoreactive cells. The high uptake of CHOL in the benign lesions in our study might be associated with the influence of simple diffusion and relatively increased metabolic activity in the reactive tissues. Additional study will be needed to establish this point. The high FDG uptake in inflammatory and benign reactive tissues is well documented.^{7-9,32}

The SUV analysis demonstrated that SUVs were lower for CHOL than FDG in malignant tumors. This observation is consistent with previous reports in patients with esophageal cancer, gynecologic cancer and lung cancer.^{18,30,33} A significant positive correlation between SUVs of CHOL and FDG ($r = 0.677$, $p = 0.004$, $n = 45$) was found in this study. The mean SUVs between malignant and benign lesions showed statistically significant differences with both CHOL and FDG. Although some overlap of SUVs was observed in this series, CHOL demonstrated somewhat better differentiation than FDG between malignant and benign lesions (Fig. 5a). This indicates that the diagnostic performance of CHOL PET may be as good as that of FDG PET in head and neck oncologic imaging. Depending on the purpose of a study, SUVs with different cutoff levels can be used to achieve very high sensitivity or specificity. In this study, the SUV cutoff value for differentiating malignant tumors from benign lesions was set to derive the highest specificity without significant effect on sensitivity. Although SUV analysis provided no significant additional advantage in the differentiation of malignant from benign lesions compared with visual interpretation in this series, we think that quantification of tumor tracer uptake in the form of SUV may complement visual image interpretation because it provides objective criteria for differentiation of malignant from benign lesions, thus minimizing interobserver variability in image interpretation. Moreover, SUV assessment may support for the diagnosis of borderline cases at visual analysis and in comparison of sequential scans. In this series, CHOL showed high uptake in all but one of the malignant tumors. From this view point, we can assume that low uptake of CHOL in a lesion may prevent unnecessary surgery or invasive biopsy procedure depending on clinical assessment, but this has yet to be validated by large correlative studies.

As compared with FDG, CHOL PET scanning has the advantage of providing good contrast images at an earlier period.¹⁷⁻¹⁹ In FDG PET imaging, patients have to wait for 50–60 min after FDG injection for scanning to reach an optimum tumor-to-background activity ratio because of its relatively slower clearance from the circulation. For CHOL, however, the retention time in the circulation is very short and tumor radioactivity reaches a maximum at 3–4 min after intravenous administration which facilitated acquisition after 5 min. The tissue-to-background radioactivity ratio remains essentially constant for more

than 30 min after the initial high uptake.^{12,19} By starting PET imaging 5 min after injection of CHOL, tumors were well visualized resulting in reduced unpleasantness for the patients who had fasted in the morning of the day of examination. Furthermore, since CHOL uptake in muscle is low,^{19,34} CHOL PET is capable of providing good contrast image, particularly in the neck where physiologic uptake of FDG in muscle sometimes causes difficulty in image interpretation. As there was no diabetic patient in our study, we could not show the superiority of CHOL over FDG imaging in patients with hyperglycemia. But some other studies have described that CHOL PET can clearly detect malignant tumors even at high serum glucose levels where FDG PET is less sensitive.³⁰

The short half-life of ¹¹C ($t_{1/2} = 20$ min) may be considered as a limiting factor for CHOL PET to acquire a whole-body image by the standard acquisition protocol. However, half-life duration is less of a limiting factor provided with an on-site cyclotron facility, and whole body (from head to pelvis) PET imaging is possible with a relatively high dose of CHOL.^{19,22} Moreover, metastasis is rarely seen below the mid thigh even in advanced stage malignancy especially in head and neck cancer.

The relatively high and variable physiologic uptake of CHOL in the salivary glands (parotid, submandibular and sublingual glands) makes it difficult to adequately interpret PET images in these organs. On the other hand, FDG also accumulates physiologically in the Waldeyer's ring, tongue and salivary glands.³⁵ The highest average metabolic activity of FDG in the salivary glands and lymphoid tissues of Waldeyer's ring has been demonstrated by Jabour et al.³⁶ Therefore, knowledge of the relative metabolic variations in the normal structures of the head and neck for both tracers is essential during interpretation of the PET images for correct diagnosis. According to some investigators, landmarks like the salivary glands may make it easier to localize the tumor on PET images.³⁵ However, increased tracer uptake in some of the benign salivary gland lesions caused most of the false-positive findings in our study with both CHOL and FDG. The availability of recent integrated PET/CT will improve the confidence of image interpretation and relatively fast acquisition.³⁷ PET/CT can help to distinguish malignant lesions from physiologic tracer uptake in normal tissues, because on the coregistered CT image, this uptake will be localized within normal-appearing tissues. Therefore, the specificity will be improved with the help of structural information provided by CT.

In conclusion, these preliminary findings indicate that the use of CHOL PET may be feasible for head and neck tumor imaging. PET imaging with CHOL seems to be able to detect malignant head and neck tumors as effectively as FDG, because of closely related tracer uptake pattern in the lesions. Therefore, both techniques are considered to have clinical value for the noninvasive diagnosis of head and neck cancer. However, both tracers

have some limitations, particularly in salivary gland lesions which emphasizes the need for further evaluation of large populations to determine the role of CHOL PET in the diagnosis of head and neck malignancy.

ACKNOWLEDGMENTS

We are grateful to Prof. Tomio Inoue and Dr. Shingo Hamaguchi, Department of Radiology, Yokohama City University Hospital, Yokohama, Japan for their advice and help with the experimental design. We thank Dr. Katsumi Tomiyoshi, Director, Radiopharmaceutical Division, Nishidai Clinic, Tokyo, Japan for his kind assistance in radiotracer synthesis. We also thank Dr. Yosiaki Sasazawa, Department of Public Health, Gunma University School of Medicine, Gunma for his assistance with the statistical analysis.

REFERENCES

1. Panje WR, Namon AJ, Vokes E, Haraf DJ, Weichselbaum RR. Surgical management of the head and neck cancer patient following concomitant multimodality therapy. *Laryngoscope* 1995; 105: 97–101.
2. Nowak B, Di Martino E, Janicke S, Cremerius U, Adam G, Zimny M, et al. Diagnostic evaluation of malignant head and neck cancer by F-18-FDG PET compared to CT/MRI. *Nuklearmedizin* 1999; 38: 312–318.
3. Scott AM. Current status of positron emission tomography in oncology. *Int Med* 2001; 31: 27–36.
4. Hannah A, Scott AM, Tochon-Danguy H, Chan JG, Akhurst T, Berlangieri S, et al. Evaluation of ¹⁸F-fluorodeoxyglucose positron emission tomography and computed tomography with histopathologic correlation in the initial staging of head and neck cancer. *Ann Surg* 2002; 236: 208–217.
5. Gallagher BM, Fowler JS, Guttererson NI, MacGregor RR, Wan CN, Wolf AP. Metabolic trapping as a principle of radiopharmaceutical design: some factors responsible for the biodistribution of [¹⁸F] 2-deoxy-2-fluoro-D-glucose. *J Nucl Med* 1978; 19: 1154–1161.
6. Baillet JW, Abemayor E, Jabour BA, Hawkins RA, Ho C, Ward PH. Positron emission tomography: a new, precise imaging modality for detection of primary head and neck tumors and assessment of cervical adenopathy. *Laryngoscope* 1992; 102: 281–288.
7. Yasuda S, Shohtsu A, Ide M, Takagi S, Ogawa J, Mitomi T, et al. High fluorine-18 labeled deoxyglucose uptake in sarcoidosis. *Clin Nucl Med* 1996; 21: 983–984.
8. Kubota R, Yamada S, Kubota K, Ishiwata K, Tamahashi N, Ido T. Intratumoral distribution of fluorine-18-fluorodeoxyglucose *in vivo*: high accumulation in macrophages and granulation tissues studied by microautoradiography. *J Nucl Med* 1992; 33: 1972–1980.
9. Braams JW, Pruijm J, Freling NJ, Nikkels PG, Roodenburg JL, Boering G, et al. Detection of lymph node metastases of squamous cell cancer of the head and neck with FDG-PET and MRI. *J Nucl Med* 1995; 36: 211–216.
10. Torizuka T, Clavo AC, Wahl RL. Effect of hyperglycemia on *in vitro* tumor uptake of tritiated FDG, thymidine, L-methionine and L-leucine. *J Nucl Med* 1997; 38: 382–386.
11. Hara T, Yuasa M. Automated synthesis of [¹¹C]choline, a

- positron-emitting tracer for tumor imaging. *Appl Radiat Isot* 1999; 50: 531–533.
12. Roivainen A, Forsback S, Gronroos T, Lehtikoinen P, Kahkonen M, Sutinen E, et al. Blood metabolism of [methyl-¹¹C]choline, implications for *in vivo* imaging with positron emission tomography. *Eur J Nucl Med* 2000; 27: 25–32.
 13. Zeisel SH. Dietary choline: biochemistry, physiology, and pharmacology. *Annu Rev Nutr* 1981; 1: 95–121.
 14. Katz-Brull R, Degani H. Kinetics of choline transport and phosphorylation in human breast cancer cells: NMR application of the zero trans method. *Anticancer Res* 1996; 16: 1375–1380.
 15. Miller BL, Chang L, Booth R, Ernst T, Cornford M, Nikas D, et al. *In vivo* ¹H MRS choline: correlation with *in vitro* chemistry/histology. *Life Sci* 1996; 58: 1929–1935.
 16. Wald LL, Nelson SJ, Day MR, Noworolski SE, Henry RG, Huhn SL, et al. Serial proton magnetic resonance spectroscopy imaging of glioblastoma multiforme after brachytherapy. *J Neurosurg* 1997; 87: 525–534.
 17. Hara T, Kosaka N, Shinoura N, Kondo T. PET imaging of brain tumor with [methyl-¹¹C]choline. *J Nucl Med* 1997; 38: 842–847.
 18. Kobori O, Kirihara Y, Kosaka N, Hara T. Positron emission tomography of esophageal carcinoma using ¹¹C-choline and ¹⁸F-fluorodeoxyglucose: a novel method of preoperative lymph node staging. *Cancer* 1999; 86: 1638–1648.
 19. Kotzerke J, Prang J, Neumaier B, Volkmer B, Guhlmann A, Kleinschmidt K, et al. Experience with carbon-11 choline positron emission tomography in prostate carcinoma. *Eur J Nucl Med* 2000; 27: 1415–1419.
 20. Hamacher K, Coenen HH, Stöcklin G. Efficient stereospecific synthesis of no-carrier-added 2[¹⁸F]-fluoro-2-deoxy-D-glucose using amino polythene supported nucleophilic substitution. *J Nucl Med* 1986; 27: 235–238.
 21. Haubrich DR, Wang PF, Wedeking PW. Distribution and metabolism of intravenously administered [methyl-³H]choline and synthesis *in vivo* of acetylcholine in various tissues of guinea pigs. *J Pharmacol Exp Ther* 1975; 193: 246–255.
 22. Pieterman RM, Que TH, Elsinga PH, Pruijm J, van Putten JW, Willemsen AT, et al. Comparison of ¹¹C-choline and ¹⁸F-FDG PET in primary diagnosis and staging of patients with thoracic cancer. *J Nucl Med* 2002; 43: 167–172.
 23. Kalra R, Wade KE, Hands L, Styles P, Camplejohn R, Greenall M, et al. Phosphomonoester is associated with proliferation in human breast cancer: a ³¹P MRS study. *Br J Cancer* 1993; 67: 1145–1153.
 24. Leskinen-Kallio S, Ruotsalainen U, Nagren K, Teras M, Joensuu H. Uptake of carbon-11-methionine and fluorodeoxyglucose in non-Hodgkin's lymphoma: a PET study. *J Nucl Med* 1991; 32: 1211–1218.
 25. Shiga T, Tsukamoto E, Nakada K, Morita K, Kato T, Mabuchi M, et al. Comparison of ¹⁸F-FDG, ¹³¹I-Na, and ²⁰¹Tl in diagnosis of recurrent or metastatic thyroid carcinoma. *J Nucl Med* 2001; 42: 414–419.
 26. Minn H, Clavo AC, Wahl RL. Influence of hypoxia on tracer accumulation in squamous cell carcinoma: *in vitro* evaluation for PET imaging. *Nucl Med Biol* 1996; 23: 941–946.
 27. Hara T, Kosaka N, Suzuki T, Kudo K, Niino H. Uptake rates of ¹⁸F-fluorodeoxyglucose and ¹¹C-choline in lung cancer and pulmonary tuberculosis: a positron emission tomography study. *Chest* 2003; 124: 893–901.
 28. Ishidate H. Choline transport and choline kinase. In: Vance DE, ed. *Phosphatidylcholine Metabolism*. Boca Raton, FL: CRC Press, 1989: 9–32.
 29. DeGrado TR, Baldwin SW, Wang S, Orr MD, Liao RP, Friedman HS, et al. Synthesis and evaluation of ¹⁸F-labeled choline analogs as oncologic PET tracers. *J Nucl Med* 2001; 42: 1805–1814.
 30. Torizuka T, Kanno T, Futatsubashi M, Okada H, Yoshikawa E, Nakamura F, et al. Imaging of gynecologic tumors: comparison of ¹¹C-choline PET with ¹⁸F-FDG PET. *J Nucl Med* 2003; 44: 1051–1056.
 31. Zhang H, Tian M, Oriuchi N, Higuchi T, Watanabe H, Aoki J, et al. ¹¹C-choline PET for the detection of bone and soft tissue tumours in comparison with FDG PET. *Nucl Med Commun* 2003; 24: 273–279.
 32. Keyes JW Jr, Harkness BA, Greven KM, Williams DW 3rd, Watson NE Jr, McGuirt WF. Salivary gland tumors: pretherapy evaluation with PET. *Radiology* 1994; 192: 99–102.
 33. Khan N, Oriuchi N, Zhang H, Higuchi T, Tian M, Inoue T, et al. A comparative study of ¹¹C-choline PET and [¹⁸F]fluorodeoxyglucose PET in the evaluation of lung cancer. *Nucl Med Commun* 2003; 24: 359–366.
 34. Zheng QH, Stone KL, Mock BH, Miller KD, Fei X, Liu X, et al. [¹¹C]choline as a potential PET marker for imaging of breast cancer athymic mice. *Nucl Med Biol* 2002; 29: 803–807.
 35. Lindholm P, Leskinen-Kallio S, Minn H, Bergman J, Haaparanta M, Lehtikoinen P, et al. Comparison of fluorine-18-fluorodeoxyglucose and carbon-11-methionine in head and neck cancer. *J Nucl Med* 1993; 34: 1711–1716.
 36. Jabour BA, Choi Y, Hoh CK, Rege SD, Soong JC, Lufkin RB, et al. Extracranial head and neck: PET imaging with 2-[F-18]fluoro-2-deoxy-D-glucose and MR imaging correlation. *Radiology* 1993; 186: 27–35.
 37. Hany TF, Schuknecht B, Schmid DT, Seifert B, von Schulthess GK, Goerres GW. In-line PET/CT in head and neck cancer patients: a comparison with FDG PET and contrast-enhanced CT. (Abstract) *Eur J Nucl Med Mol Imaging* 2003; 30: S277.